Available online at www.sciencedirect.com

SciVerse ScienceDirect

Journal of the European Ceramic Society 32 (2012) 697–704

www.elsevier.com/locate/jeurceramsoc

High *P–T* phase transformations and metastability in the $Zr_{0.5}Hf_{0.5}O_2$ solid-solution ceramic

Neil R. Jackson [a], Rudolph M. Erasmus [a], David G. Billing [b], Giovanni R. Hearne [c,*]

[a] *School of Physics and DST-NRF Centre of Excellence in Strong Materials, University of the Witwatersrand, Private Bag 3, Wits 2050, Johannesburg-Gauteng, South Africa*

[b] *School of Chemistry and DST-NRF Centre of Excellence in Strong Materials, University of the Witwatersrand, Private Bag 3, Wits 2050, Johannesburg-Gauteng, South Africa*

[c] *Department of Physics and DST-NRF Centre of Excellence in Strong Materials, University of Johannesburg, P. O. Box 524, Auckland Park, Johannesburg-Gauteng 2006, South Africa*

Received 26 May 2011; received in revised form 27 September 2011; accepted 1 October 2011
Available online 22 October 2011

Abstract

High pressure–temperature (*P–T*) phases of the $Zr_xHf_{1-x}O_2$ ($x = 0.5$) solid-solution have been stabilised in a CO_2 laser heated diamond anvil cell. At room-temperature the monoclinic to orthorhombic-I structural transformation is initiated at 5–8 GPa. The X-ray diffraction (XRD) studies show these two phases coexist to above ~15 GPa. A progressive increase in the orthorhombic-I phase abundance occurs, to culminate in full conversion at ~20 GPa. At this lower threshold of ~20 GPa transformation to the orthorhombic-II (cotunnite) structure can be initiated by heating in the range of 600–1200 °C. Substantial conversion to the cotunnite phase occurs in the same temperature range at 25–30 GPa. Raman signatures have been assigned to the two orthorhombic high-pressure phases, aided by the qualitative assessment of the complementary XRD data. Decompression experiments show that phase mixture composites of these high pressure structures, possibly with enhanced tribological properties, can be recovered to ambient conditions.

Keywords: A. Sol–gel processes; B. X-ray methods; D. ZrO_2; High pressure–temperature; Raman spectroscopy

1. Introduction

Zirconium dioxide (zirconia, ZrO_2) and hafnium dioxide (hafnia, HfO_2) are well known binary oxide materials that are used in applications for structural ceramics, high temperature solid electrodes and also as substrates for growth of other materials.[1] ZrO_2-strengthened ceramics of high hardness and toughness, with erosion and corrosion resistance, are increasingly important as refractory materials in modern industry. Other applications of these ceramics include high-*k* (high permittivity) materials for use in Ge channel materials in MOSFETS and to replace SiO_2 as the gate dielectric in CMOS technology.[2] These ceramics are also used extensively as implants for the dental industry in the form of dental caps. They are also used as optical films because zirconia based ceramics are transparent and have a high refractive index.

At ambient pressure and room temperature both ZrO_2 and HfO_2 are stable in the so-called baddeleyite or monoclinic structure (space group: $P2_1/c$). At temperatures above ~1000 °C the structure changes to tetragonal and then to the cubic fluorite structure as shown in the schematic phase diagram of Fig. 1.[3,4] The phase change from monoclinic (M) to orthorhombic-I (O-I), space group Pbca, occurs at ~5 GPa near ambient temperature. At higher pressure and at temperatures near the room temperature isotherm, there is a further phase transformation to an orthorhombic-II (O-II) structure (space group: Pnma) between 12 and 25 GPa.[5] This O-II structure with ninefold coordinated polyhedra is also known as the cotunnite phase. High temperature processing at pressure accelerates the kinetics of the O-I → O-II transition. The high-pressure stabilised O-II phase can be recovered to ambient conditions (exhibits metastability) whereas the O-I does seem to revert back to the starting M phase.[3,4] The bulk modulus of cotunnite-type ZrO_2 has been

* Corresponding author. Tel.: +27 011 5593849; fax: +27 011 5592339.
E-mail address: grhearne@uj.ac.za (G.R. Hearne).

0955-2219/$ – see front matter © 2011 Elsevier Ltd. All rights reserved.
doi:10.1016/j.jeurceramsoc.2011.10.016

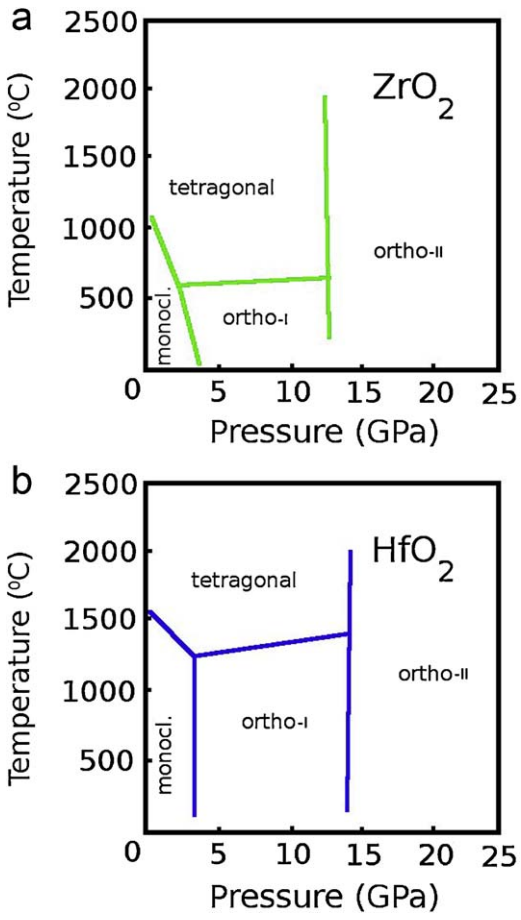

Fig. 1. Schematics of the known *P–T* phase diagrams of (a) ZrO_2 and (b) HfO_2 end members. Solid lines represent previously reported phase boundaries between monoclinic, tetragonal, orthorhombic-I and orthorhombic-II phases.

determined to be 278 GPa in experiments to very high pressures of ~100 GPa,[6] compared with the calculated value of 305 GPa.[7] The bulk modulus of HfO_2 has been determined to exceed 300 GPa.[8,9] These high values for the bulk moduli demonstrate that high pressure stabilised phases of both ZrO_2 and HfO_2 are quite incompressible. They have therefore attracted attention as candidate ultra-hard materials with important applications if they are metastable and can be recovered to ambient conditions, as confirmed some time ago.[9]

However further wide-ranging potential applications of pure ZrO_2-toughened ceramics are limited by the low monoclinic to tetragonal transformation temperature and the high pressure phases, although metastable with low compressibility values, may not have as enhanced hardness properties as originally anticipated.[5] The mechanical properties of ZrO_2-based ceramics are also strongly affected by composition and microstructure.[10] It may be noted that HfO_2 has a higher monoclinic to tetragonal transformation temperature (~1700 °C) than ZrO_2. Moreover because of the similar chemistry of the metal-ions, ZrO_2 and HfO_2 form a continuous solid-solution series of $Zr_xHf_{1-x}O_2$. Therefore HfO_2-toughened ZrO_2-derived ceramics, that is $Zr_{1-x}Hf_xO_2$ solid-solutions, have been widely considered as potential new generation "superceramics" with superior mechanical properties and tribological characteristics over that of the end-member oxides.[1,11]

Much less is known about the high pressure phases (O-I and O-II) of these solid solutions in comparison to what has been derived from quite extensive investigations of the *P–T* phase diagrams of the ZrO_2 and HfO_2 end-members.[3–6] The focus in this work is on exploring quite thoroughly the pressure–temperature response of one of these solid-solution compositions in the laser heated diamond-anvil cell (DAC), namely the midpoint in the series $Zr_{1-x}Hf_xO_2$ ($x = 0.5$). We anticipate that this will provide some guidance in future studies of the *P–T* response of other compositions in the solid-solution series.

2. Experimental

2.1. Samples

A set of zirconia–hafnia solid solutions of varying compositions ($Zr_xHf_{1-x}O_2$ with $x = 0$, 0.25, 0.5, 0.75, 1) have been synthesized by means of an organic sol–gel technique so as to obtain high quality starting materials.[12–14] The sol–gel technique ensures that highly homogeneous high purity fine powders of precursor material can be obtained at relatively low processing temperatures. Differential thermal analysis measurements demonstrated that crystallization from the amorphous sol–gel derived starting materials occurred in the range of 450–550 °C for the different compositions. Therefore these starting materials were calcined at 1000 °C for 1 h to effect crystallization of single phase monoclinic samples for each of the compositions. This was confirmed by both XRD and Raman measurements at room-temperature after the calcination processing.

Only the $x = 0.5$ sample has been selected for the high *P–T* experiments. The lattice parameters of the monoclinic unit cell of the $Zr_{0.5}Hf_{0.5}O_2$ powder was obtained as $a = 0.5132 \pm 0.0013$ nm, $b = 0.5200 \pm 0.0014$ nm $c = 0.5300 \pm 0.0014$ nm and unit cell angle $\beta = 99.9° \pm 0.4°$. The unit cell volume (0.1414 nm^3) is situated on the trend line of a monotonically decreasing unit cell volume in going from the monoclinic ZrO_2 end-member through to HfO_2.[15] The Raman spectra of these samples are also consistent with published characterisation data of these systems. [16,17]

Field emission scanning microscopy (SEM) has been used to determine particle size and morphology. The full width at half maximum, after corrections for strain, for $(\bar{1}\,1\,1)$ and $(1\,1\,1)$ Bragg reflections in the XRD patterns have also been used to estimate particle size. The SEM micrographs show particles to be more or less spherical with diameters of less than 100 nm for all the solid-solution compositions. The micrographs also indicate that as a result of the calcination, primary particles start to sinter together resulting in the formation of agglomerates. The XRD analysis confirms the average grain size of the primary particles to be ~50 nm diameter.[12]

2.2. DAC pressure aspects

A number of separate *P–T* experimental runs were conducted on the sample. In a pressure study to ~20 GPa, involving no

heating, fluorinert FC70/FC77 (1:1) has been used as the pressure transmitting medium (PTM). Our tests have shown this gives a sufficiently low background signal in Raman experiments although it does not remain completely hydrostatic. In other runs where laser heating was effected, Ar gas has been liquefied and cryogenically loaded into the sample cavity as the PTM.[18]

A miniature Merrill-Basset-type diamond anvil cell (MB-DAC) has been used to generate pressure. This has been loaded with a Boehler-Almax anvil (550 μm culet beveled to 650 μm at an 8° angle), mounted in a 70° exit-cone aperture of a WC backing plate on the exit side of the DAC. This is important for the XRD pressure studies to ensure the widest possible range of diffraction angle, 2θ. A standard brilliant cut anvil of similar culet dimensions has been used on the entrance side of the DAC. Diamond anvils in all cases were Type-Ia. A stainless steel (SS301) gasket of ∼200 μm starting thickness has been pre-indented to 40–50 μm and a ∼200 μm diameter cavity drilled by the spark erosion technique. We have also used a miniature piston-cylinder DAC with a Re gasket and sample cavity of ∼150 μm diameter in a separate Raman experiment to higher pressures of ∼30 GPa.

One or two tiny ruby balls or fragments have been loaded at convenient locations in the cavity and pressure is evaluated at room temperature by using the standard ruby fluorescence technique.[19] The home-built system is comprised of an Olympus BX-60 compound microscope, 20 mW 532 nm green laser excitation source and Ocean-Optics HR4000CG spectrometer coupled by an optic fibre to the trinocular turret of the microscope.

Powdered sample was then loaded into the gasket indentation and pressed into thin transparent flakes of 10–15 μm thickness and then pushed into the sample cavity, see Fig. 2. Such thin flakes minimise the chance of contact with the diamond anvil culet face when the Ar PTM is loaded. The Ar fluid serves to insulate the sample from the highly thermally conductive anvil so that high temperatures may be sustained by the sample upon laser heating. The flake is also thin enough to ensure high transmittance of the laser beam so as to avoid uncontrolled over-heating of the sample far in excess of 1000 °C where the laser spot impinges. This high transmittance also ensures that there are no significant axial temperature gradients extending though the depth of the sample at the laser hot spot.

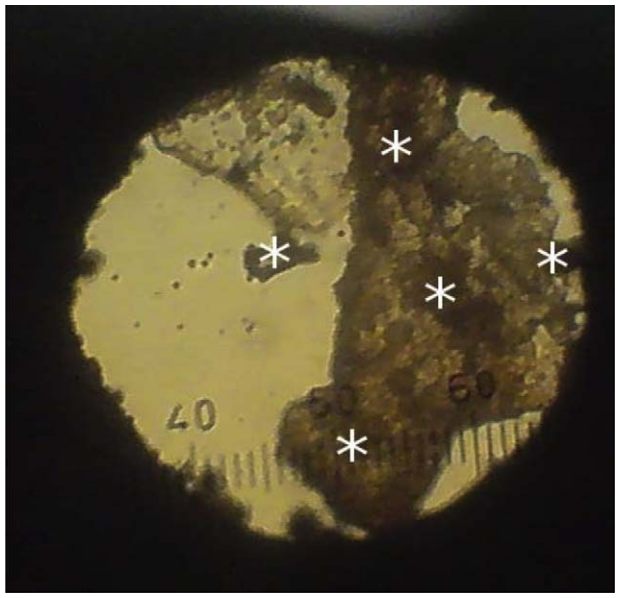

Fig. 2. DAC cavity at 2 GPa loaded with thin flakes of $Zr_{0.5}Hf_{0.5}O_2$, sample and Ar pressure transmitting medium (PTM). Cavity dimensions are 200 μm diameter drilled in a stainless steel (SS301) gasket, viewed in transmitted light. The transparency of the flakes is indicative of the thickness $t \approx 10$–15 μm through which much of the CO_2 laser heating radiation is transmitted. Small ruby balls for manometry may be discerned in the bottom half of the cavity. Asterisks indicate regions probed by Raman spectroscopy.

2.3. Laser heating

The laser heating system comprises a 30 W quasi-continuous wave CO_2 laser (Synrad model), the beam of which is focussed into the sample cavity to a spot size of 20–50 μm FWHM by means of appropriate ZnSe optics and copper mirrors. Details of the facility have been published elsewhere.[20] With this set-up 220× magnification of the image of the sample cavity is attained for viewing on a monitor after it is projected onto a CCD camera sensor element. Most of the beam is transmitted through the thin pressurised flake of sample. Therefore a second CCD camera is installed on the sample (DAC) stage to monitor the transmitted laser beam traversing through the sample cavity and sample flake. This arrangement provided a modest magnification of about 10× of the transmitted beam. The DAC is mounted on a sample stage which is water cooled to avoid heat damage to the type-Ia diamonds that have high thermal absorption at the 10.6 μm laser wavelength (this can be as high as 70% for a type-Ia anvil window 2 mm thick).[20] Even when operating the laser at full power no visible emission has ever been obtained from the sample surface because of the high transmittance of the thin flake. The CCD camera at the exit aperture helped to verify that the laser beam was indeed being transmitted through the sample. The absence of emission in the visible regime is taken to be an indication that temperatures did not exceed ∼1200 °C.[20] During heating experiments we attempted to focus beyond the sample into the exit anvil (after absorption by the sample flake). This was to avoid local heating damage that may have resulted from focussing effects if the focal point was in the entrance anvil.

2.4. High pressure Raman spectroscopy

A Jobin-Yvon T64000 Micro-Raman spectrometer has been used. This comprises a BX40 Olympus microscope attachment, holographic gratings (1800 grooves mm^{-1}), a liquid nitrogen cooled CCD detector, 514.5 nm line of Ar^+ laser used as an excitation source and the spectrometer has been operated in the triple-subtractive mode. The entrance slit width of the pre-monochromator was set at 150 μm. The diameter of the laser spot at the sample was 5–10 μm. The confocal pinhole was set to between 100 and 200 μm to reduce the depth of the focal plane region as much as possible so as to minimise sampling background signal from the anvil. Under these conditions data

acquisition times for each spectrum was 5–10 min in the case of the laser heated MB-DAC. Estimated power at the entrance aperture of the DAC was less than 10 mW. In the cases of laser heating, micro-Raman measurements were made on the quenched samples still at pressure in the DAC. We could selectively sample regions that were left unheated and separately sample those regions where the CO_2 laser heated spot was made to impinge on the sample.

2.5. Laboratory based XRD high pressure studies

XRD data has been taken at pressure on laboratory based instruments using a Bruker SMART diffractometer equipped with a 1K CCD detector. This comprised a conventional X-ray generator and Mo–K_α radiation ($\lambda = 0.71073$ Å). The collimated beam is directed normal to the table of the entrance anvil by means of a 0.1 mm aperture monocapillary.[21] The DAC has been mounted on a customised x–y–z stage that permits its optimal alignment with the exit of the monocapillary. Angle-dispersive diffraction patterns were in the form of Debye-Scherrer rings recorded on the 512 × 512 pixels of the area detector.

Two 30 min dark field measurements were taken, averaged and automatically subtracted out of the powder ring pattern using SMART-NT software.[22] Once the ring pattern had been collected SMART-NT software was used to unwarp the rings and the powder ring pattern imported into the FIT2D software package for further data processing.[23] This program has been used to convert 2-dimensional powder ring patterns into intensity-versus-2θ powder patterns. The background was subtracted using a standard program, WinPLOTR,[24] and the peaks were identified and labelled manually. XRD patterns shown in Fig. 3 onwards are such background corrected patterns.

3. Results and discussion

Fig. 3(a) shows pressure evolution of XRD patterns of $Zr_{0.5}Hf_{0.5}O_2$ loaded in the MB-DAC. The monoclinic (M) phase (at 0.6 GPa, sealing pressure) clearly shows two signature peaks at 12.5° and 14°, measured in 2θ, labelled as the (1 1 −1) and (1 1 1) reflections, respectively. This is taken from the corresponding peaks of the end members.[3–5] The reflection signatures in the range of 12°–15° are primarily used for identification of the M phase. As pressure rises above 4.7 GPa, peaks at 12.5° and 14° decrease in intensity and a new peak evolves in between these at 13° indicative of an O-I phase occurring. This O-I signature is evident in the XRD pattern at 8.2 GPa of Fig. 3(a). There are additional signature peaks at 16° and 22° of the O-I phase, in analogy to the end members.[3–5].

This confirms that the M to O-I phase boundary is in the 5–8 GPa region, similar to the end members (see Fig. 1). Besides the above mentioned signature reflections of the M and O-I phases, there are also other associated combinations of Bragg reflections from the sample which are, of low intensity, broad and not readily distinguishable. The behaviour of the low angle reflections in Fig. 3(a) indicates that, although the M to O-I phase change is initiated at ∼5 GPa, the starting M phase dominates up to the regime of 8–11 GPa. There is thus phase coexistence of starting M and high pressures O-I structures from 5 to 8 GPa onwards. The highest intensity O-I peaks are at ∼13.5° (labelled the (2 1 1) reflection) and ∼16° (combination of the (0 2 0), (0 0 2) and (4 0 0) reflections).

This phase coexistence behaviour in the solid-solution seems to be similar to that of the end-members. Measurements at low pressure of ZrO_2 also show a sluggish phase transformation and a mixture of phases over a wide range of pressures at room

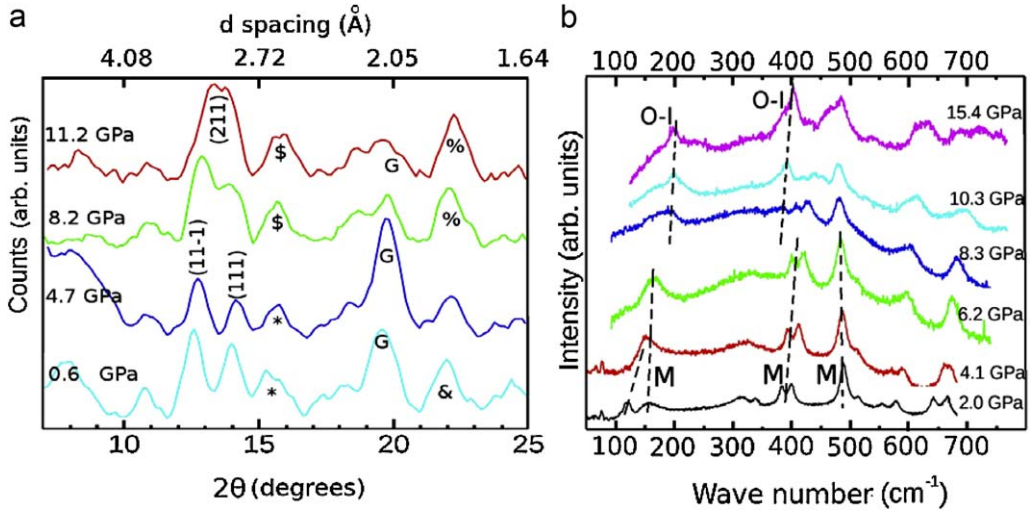

Fig. 3. (a) XRD patterns as a function of scattering angle 2θ of the $Zr_{0.5}Hf_{0.5}O_2$ sample at pressure in the MB-DAC (fluorinert PTM). Corresponding d-spacing labels are included on the top axis for convenient comparison with some cases of previous literature on the end members. The two prominent peaks at 12.5° (1 1 −1) and 14° (1 1 1) are the most intense reflections from the M phase. At 8.2 GPa the most intense O-I reflection, (2 1 1) at 13.5°, is discerned. The prominent peak at ∼20° (G) is from the gasket (more intense when the DAC is not well aligned). The symbol * refers to a combination of (0 2 0) and (2 0 0) reflections in the M phase. Symbol $ is a combination of, (0 2 0), (0 0 2) and (4 0 0) reflections of the O-I phase. Other symbols, & and %, are combinations of reflections explained in the text where appropriate. These combinations of reflections at 2$\theta \geq 15°$ are deduced from comparison with the XRD patterns of the end member compositions. (b) Raman spectra of $Zr_{0.5}Hf_{0.5}O_2$ at pressure in Ar PTM before laser heating. Dashed lines delineate conspicuous signature peaks in the M and O-I phases.

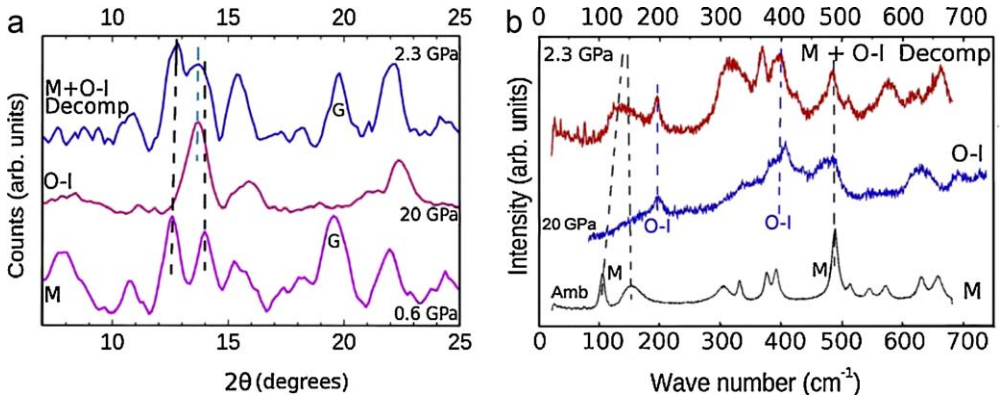

Fig. 4. (a) XRD patterns taken upon decompression from 20 GPa (fluorinert PTM) down to 2.3 GPa. The data at 0.6 GPa (close to ambient) is the monoclinic (M) structure at the start of the compression sequence. The top pattern is the end of the decompression sequence from the highest pressure of 20 GPa. At 20 GPa the majority phase, if not all of the sample, is in the O-I structure. The decompression pattern at 2.3 GPa is a mixture of M (higher percentage) and O-I phases. (b) Corresponding Raman spectra highlighting the signature M and O-I Raman bands. These figures indicate that a mixture of M and O-I phases occur at near ambient conditions after decompression from 20 GPa.

temperature.[4] In that work on ZrO_2 it is indicated that the M phase coexists with the O-I phase up to a pressure of ~15 GPa.

The sample was left for several days upon further pressurisation of the $Zr_{0.5}Hf_{0.5}O_2$ sample to ~11 GPa. There appears to have been a further evolution of the O-I phase over several days after initiating the M → O-I transformation. This suggests that the kinetics of the O-I transition is perhaps on a time scale of days at room-temperature.

The pressure evolution of Raman spectra of the $Zr_{0.5}Hf_{0.5}O_2$ sample is depicted in Fig. 3(b). Raman spectra were taken on the darker (thicker) regions of the sample, in an MB-DAC prepared for anticipated laser heating studies at pressure, due to a better signal to noise ratio in those areas (labelled with asterisks in Fig. 2). The pressure evolution of the $Zr_{0.5}Hf_{0.5}O_2$ sample may be compared with a separate Raman pressure experiment on the end members.[8] Under ambient conditions the prominent Raman bands of the M phase range from 100 cm^{-1} through to 700 cm^{-1}. Fig. 3(b) delineates key Raman signatures of the M phase, at 100–150 cm^{-1}, a doublet at ~400 cm^{-1} and a strong band at ~500 cm^{-1}. These can be clearly discerned up to ~6.2 GPa. When the pressure is increased further to ~8 GPa a different Raman signature seems to evolve at ~200 cm^{-1} and there are relatively strong unresolved bands at ~400 cm^{-1} and 500 cm^{-1}. The bands at these higher pressures are distinctly broader than those of the low pressure monoclinic phase. Taken in conjunction with the behaviour of the XRD patterns in Fig. 3(a), Raman spectra in Fig. 3(b) at $P > 6.2$ GPa indicate the conspicuous signature bands of the O-I phase.

The sluggishness of the transition from the M to O-I structure at room temperature and consequent M/O-I phase coexistence initiated in the 5–8 GPa regime is thus seen in both the complementary XRD and Raman data sets of Fig. 3. The O-I phase is not fully stabilised (although it may be the majority phase) at ~15 GPa consistent with the literature on ZrO_2,[3,4] until pressure is increased to ~20 GPa, see Fig. 4. The Raman spectra at ~15 GPa and above, Figs. 3 and 4, may thus be considered as a reference for the Raman signatures of the O-I phase. In particular, O-I signature bands at 200 and 400 cm^{-1} will be referred to again later when further conversion to the O-II phase is considered after heating experiments at higher pressure $P \geq 20$ GPa.

Fig. 4 also shows the XRD and Raman spectra of the sample (in fluorinert PTM) after it has been fully converted to the O-I phase at ~20 GPa and then decompressed to near ambient conditions. The pressure has been decreased in small steps from 20 GPa down to ~2 GPa. At the lowest decompression steps the DAC was immersed in a bath of liquid nitrogen to attempt to quench in the O-I phase (it is much more difficult to recover the sample intact to ambient conditions with this procedure). Consideration of the XRD data in Fig. 4(a) and the Raman spectra in Fig. 4(b) suggest that a mixture of phases occur in the sample recovered to 2 GPa. In the XRD data the two M signature reflections at 12.5° and 14° reappear and the O-I peak is discernible between these two peaks at ~13°, see Fig. 4(a). Raman modes from the M structure as well as O-I phase are discernible, see Fig. 4(b). This shows that there is some reversion to the original M phase.

In previous investigations, micro-indentation tests on the end member ZrO_2 suggest that a M/O-I mixed phase is a tougher material compared with the starting M phase.[25] In future experiments it may be worthwhile to check for such enhanced characteristics of the recovered phase mixtures (Fig. 4) of the $Zr_{0.5}Hf_{0.5}O_2$ solid-solution and related compositions as well.

Having rationalised the behaviour of the sample up to ~20 GPa along the room temperature isotherm, we have then progressed to (laser) heating the pressurised sample. In a separate experiment using Ar PTM, the solid-solution sample has been progressively pressurised to 20 GPa to effect full conversion to the O-I phase. There is no expectation of the O-II phase as confirmed by the absence of its anticipated signature peaks at ~15° and ~20° with no heating applied, see Fig. 5.[4,5]

The sample was then laser heated by scanning the hot-spot over the entire contents of the cavity for a period of about an hour. Our technique, previously described in the experimental section, ensures that we can establish that the laser beam is transmitted through the contents of the thin flakes that constitute the sample in the pressurised cavity. At no point was Planck

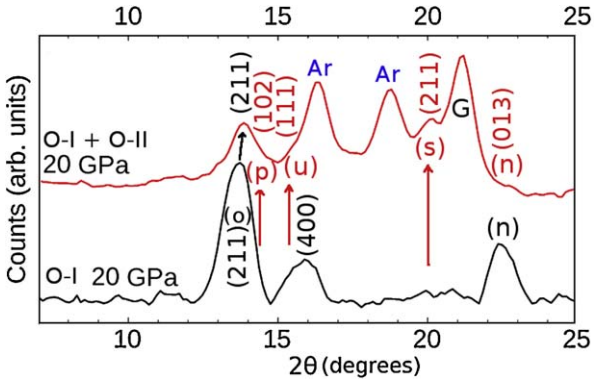

Fig. 5. Comparison of XRD spectra at 20 GPa in different pressure runs, including the quenched sample after laser-heating at 20 GPa in Ar PTM (upper pattern). Lower pattern at 20 GPa with fluorinert PTM involved compression only and no heating. The arrows show where indications of signature O-II peaks ((p), (u), (s)) are discerned as deduced from the ZrO_2 and HfO_2 end members. The solid Ar reflections are also labelled. Note that the peak (n) is much less intense in the pattern of the laser heated sample, as further indication of the initiation of a phase transformation of O-I → O-II upon heating at 20 GPa.

emission in the visible spectral range discerned from the sample because of the high transmittance of the thin flakes. Therefore it is estimated that high temperatures were restricted to the range of 600–1200 °C. Referring to the XRD data of the laser heated sample in Fig. 5 then shows that a (2 1 1) O-I signature reflection at about 14° (marked (o)) overlaps an, anticipated relatively weak, O-II (0 1 1) reflection. At slightly higher 2θ values there are two shoulder features denoted (p) and (u). These are considered to be signature O-II reflections, (1 0 2) and (1 1 1), as identified in the end member XRD patterns.[3–5] The peak denoted (s) at ∼20°, (2 1 1) reflection, is also a signature peak of the O-II phase. This (2 1 1) reflection is the most intense feature of the O-II phase of the end members.[3–5] Therefore the presence of the two shoulder features on either side of 15° and the (2 1 1) reflection at ∼20° are compelling indications of the presence of the O-II phase as a result of the laser heating. The Ar PTM peaks are labelled (q) and (r), and mask any O-II peaks in that region. The SS301 gasket peak (G) at 21° is also identified. Also note that the unresolved reflections labelled (n) occur in the monoclinic and O-I phases and there is a substantial decrease in the relative intensity of this feature in the laser heated sample, see Fig. 5. This is taken to signify a phase transformation of the O-I structure (to that of the O-II phase) upon heating at ∼20 GPa.

Features of the O-I phase are still present in the XRD spectrum at 20 GPa of the laser heated sample, seen by comparing the patterns in Fig. 5. The feature (o) is the (2 1 1) signature O-I reflection, previously seen to emerge between M phase reflections (at 12.5° and 14°) in the data at 8.2 GPa (Figs. 3 and 4). Thus the relatively weak O-II (0 1 1) reflection expected to be near this position is overlapped by the O-I (2 1 1) reflection, denoted (o). It is also indicated, in the end members, that this sluggishness may be overcome by heating at temperatures above 600 °C.[3,4] As such it is believed that at 20 GPa in the laser heated sample there is a mixture of O-I and O-II phases. This has also been confirmed by our Raman measurements (not shown) where O-I signature bands (∼200 and 400 cm^{-1}) prevail in the laser

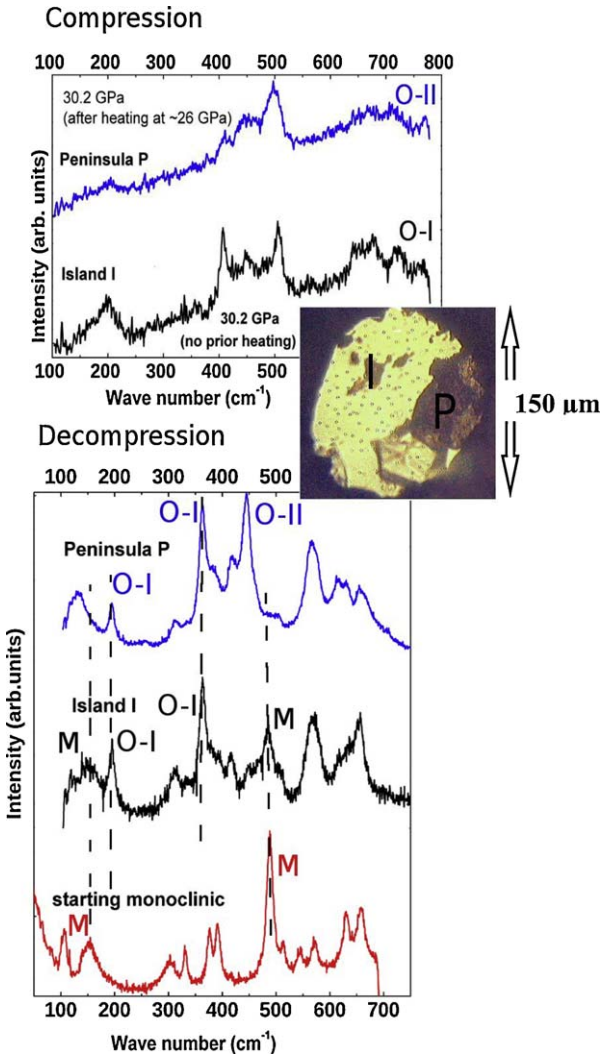

Fig. 6. Inset photo shows the readily distinguishable island I and peninsula P regions of the pressurised sample (Ar PTM). Ruby flake for manometry is visible in the lower part of the cavity adjacent to P. Compression panel shows Raman spectra of the $Zr_{0.5}Hf_{0.5}O_2$ sample at ∼30 GPa, after the peninsula region of the sample was selectively heated at a prior compression value of ∼26 GPa. The island region was left unheated throughout compression to the highest pressure and show features of O-I phase predominance, from signature Raman bands discerned at 200 and 400 cm^{-1}. Both the absence of a prominent band at ∼200 cm^{-1} and marked reduction in relative intensity at 400 cm^{-1} in the peninsula as well as the envelope features at 400–500 cm^{-1}, are indicative of conversion to an O-II majority phase from the heating. Bottom panel shows Raman spectra of these regions upon decompression to ambient conditions. Dashed lines are to highlight signature bands of various structures in the phase mixtures (discussed in the text).

heated sample at 20 GPa. The full conversion to O-II can likely be accelerated with longer heating times in this low temperature regime of 600–1200° C at this pressure. An important finding of this work is that it appears there first has to be full conversion to the O-I phase (by compression to ∼20 GPa) in the solid solution, before heating will accelerate the kinetics of transformation to the O-II phase at pressures of ∼20 GPa and above.

Fig. 6 shows Raman data obtained in a separate run to as high as ∼30 GPa. In this case certain regions of the sample (so-called peninsula P) were selectively laser heated at pressures

beyond ~20 GPa. Other regions (island I) were left completely unheated to the highest pressure of ~30 GPa. In this way an inter-comparison of heated and unheated regions of sample could be made, to ascertain the effects of heating at pressures beyond when transformation to the O-I phase was completed at ~20 GPa. Recollection of the analyses in Figs. 3 and 4 suggests that the island region at ~30 GPa exhibits the conspicuous O-I signature bands at ~200 and 400 cm^{-1} as well as a feature at ~500 cm^{-1} (see lower spectrum of the compression panel in Fig. 6). This then appears to be predominantly O-I phase. We cannot discount that intensity in this 400–500 cm^{-1} region overlaps signatures of the O-II phase, since the pressure-transformed O-II phase is known to occur along the room temperature isotherm (no heating) of the end members.

The spectrum of the laser heated P region (upper pattern at ~30 GPa) has prominent bands in the range of 400–500 cm^{-1}, similar to the O-II phase of the ZrO_2 and HfO_2 end members.[8,9] The Raman band found at 100–200 cm^{-1} in the O-II phase of the end members,[8,9] is absent or is of much lower relative intensity in the O-II phase of the solid-solution. Note also that the signature Raman bands at 200 and 400 cm^{-1} identified in the O-I phase of the solid solution (island region) are absent or much less prominent in the laser-heated region P. This is interpreted as further evidence of the O-I → O-II phase conversion as depicted in the comparison of compression Raman spectra of Fig. 6.

Therefore, Fig. 6 permits a comparison of Raman spectra involving laser-heating of the solid-solution at pressures higher than 20 GPa with Raman spectra of O-II phases of the end members, as well as our unambiguous identification of the Raman finger-print of the O-I phase of the $Zr_{0.5}Hf_{0.5}O_2$ solid-solution (Figs. 3 and 4). This inter-comparison, supported by our XRD results, suggests that in the pressure run to ~30 GPa there was significant conversion to the O-II phase upon laser-heating at 26 GPa (where laser heating was first effected) of a region of the thin flake in which temperatures did not exceed ~1200 °C (no visible emission from the laser hot-spot).

After the sample had been taken to the highest pressure of 30 GPa, decompression studies were undertaken so as to check for metastability of the high pressure phases. The panel on decompression data in Fig. 6 shows Raman spectra of the sample recovered to ambient conditions plotted together with the Raman pattern of the original M phase.[16] The spectra of regions of the recovered sample are clearly different from that of the sample in the starting M structure. There is a relatively prominent band at ~500 cm^{-1} in the recovered island region, I, which is typical of the original monoclinic M phase. Note this signature does not appear in the recovered laser heated P region. The O-I signatures at ~200 cm^{-1} and ~360 cm^{-1}, having the anticipated mode softening to these lower wave numbers from values at high pressure, also occur in the recovered island region. Therefore the unheated pressurised island region is recovered to ambient conditions as a mixture of M and O-I phases. The peninsula is the region that had been subjected to prior heating at ~26 GPa. There is a strong signature band at ~450 cm^{-1}, attributable to the O-II phase, as well as other intensity features in that region. There are also O-I signature bands at ~200 cm^{-1} and ~360 cm^{-1}. The relative intensities of all these signature bands (and comparison with the recovered island region) are compelling indications that the O-II phase is locked in to ambient conditions, as in the end members.[8,9] Therefore the laser-heated peninsula, which is predominantly O-II at 30 GPa, has a mixture of O-II and O-I phases when recovered to ambient conditions.

4. Conclusions

The monoclinic phase of the solid-solution ceramic $Zr_{0.5}Hf_{0.5}O_2$ has been synthesized by a sol–gel technique and calcination of the precursor phase at 1000 °C. Agglomerated material with spherical constituent grains of ~50 nm diameter have been obtained and subjected to high *P–T* investigations.

The laboratory-based XRD pressure experiments of this work have confirmed that the monoclinic to O-I phase transition is sluggish at room temperature. The O-I phase initiated in the range of 5–8 GPa is only fully stabilised at ~20 GPa. It may be desirable to quench such M/O-I phase mixtures, that occur above 5 GPa, to ambient conditions and to consider the mechanical and tribological properties of such composites. Laser heating at ~20 GPa initiates the conversion of the sevenfold coordinated O-I structure to the ninefold coordinated O-II phase. It is anticipated that protracted heating (hours) at modest temperatures 600–1200 °C of the $Zr_{0.5}Hf_{0.5}O_2$ solid-solution will fully convert the O-I to the O-II phase. Heating to higher temperatures has the risk of converting to other unidentified high *P–T* phases as in the case of the end-members.[4] Alternatively at higher pressures in the range of 20–30 GPa (laser) heating at 600–1200 °C for tens of minutes accelerates the phase conversion to O-II.

Key Raman signatures of the O-I and O-II high pressure phases of the solid-solution have been identified for the first time as aided by the complementary XRD pressure studies. In regions of sample taken to ~30 GPa and recovered to ambient conditions, a phase mixture is obtained that partly contains a high-pressure structural O-I (and M) phase or both O-I and O-II phases, depending on whether there has been heating at pressure or not. Therefore the O-I and O-II high pressure phases of the solid solution are shown to both be metastable. The recovered phase mixtures ought to have enhanced tribological properties of a hardened–toughened composite,[25] although one of the phase mixture combinations (O-I/O-II) originates from extreme *P–T* in the range of 20–30 GPa. This perhaps merits further detailed investigation, as well as studies of the metastability of high *P–T* phases in the other solid-solution compositions of $Zr_xHf_{1-x}O_2$ as well.

The main benefit of the qualitative XRD and Raman characterisation studies are, that regimes of the *P–T* phase diagram of the $Zr_{0.5}Hf_{0.5}O_2$ solid-solution are perhaps now better understood. The *P–T* phase diagram of the solid solution is similar to that of Fig. 1(b) (end member HfO_2) except that the two (near) vertical phase boundaries have shifted to ~5 GPa for the onset of the M → O-I transition and to ~20 GPa for the onset of the O-I → O-II transition. Therefore the low pressure phases appear to be stabilised to somewhat higher pressures than in the end-members. There is less certainty about the near horizontal high temperature phase boundaries. Studies at ambient pressure[15] and our selected laser heating experiments at high pressure suggest

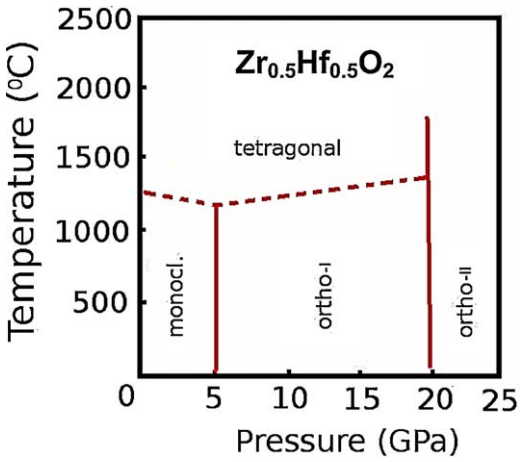

Fig. 7. Preliminary phase diagram of the $Zr_{0.5}Hf_{0.5}O_2$ solid solution for comparison with the end members. There is less certainty about high temperature phase boundaries and these have rather been depicted as dashed lines.

they are similar to Fig. 1(b). All of this information is depicted in the preliminary phase diagram of Fig. 7 which may be compared with that of Fig. 1. Moreover the O-I phase is metastable, unlike the case of the end members. These changes in comparison to the end members are attributable to disorder induced effects in the solid-solution lattice.

To the best of our knowledge this is the first high *P–T* investigation of a solid-solution in the series $Zr_xHf_{1-x}O_2$. As such it provides valuable guidance of what *P–T* regimes to work in, for example, in future synchrotron XRD studies. The latter will permit a quantitative analysis to be made of pressure–volume data such that important quantities like the bulk modulus (compressibility) of the high pressure phases may be extracted as well as a detailed mapping of the *P–T* phase diagram.[4,5]

Acknowledgments

The support of the DST-NRF Centre of Excellence in Strong Materials (CoE-SM) towards this research, including an MSc scholarship to NJ, is hereby acknowledged. Dr Emela Mochubele (née Mojaki) contributed in the initial stages of this work as part of her PhD research. F.R.L. Schoning provided crucial expertise in the XRD experiments.

References

1. Wang J, Li HP, Stevens R. Hafnia and hafnia-toughened ceramics. *J Mater Sci* 1992;**27**:5397–430.
2. Kamata Y. High-*k*/Ge mosfets for future nanoelectronics. *Mater Today* 2008;**11**:30–3.
3. Ohtaka O, Fukui H, Kunisada T, Fujisawa T, Funakoshi K, Utsumi W, et al. Phase relations and volume changes of hafnia under high pressure and high temperature. *J Am Ceram Soc* 2001;**84**:1369–73.
4. Ohtaka O, Fukui H, Kunisada T, Fujisawa T, Funakoshi K, Utsumi W, et al. Phase relations and equations of state of ZrO_2 under high temperature and high pressure. *Phys Rev B* 2001;**63**:727–33.
5. Al-Khatatbeh Y, Lee KKM, Kiefer B. Phase relations and hardness trends of ZrO_2 phases at high pressure. *Phys Rev B* 2010;**81**:214102–11.
6. Ohtaka O, Andrault D, Bouvier P, Schultz E, Mezouar M. Phase relations and equation of state of ZrO_2 to 100 GPa. *J Appl Cryst* 2005;**38**: 727–33.
7. Dewhurst JK, Lowther JE. Highly coordinated metal dioxides in the cotunnite structure. *Phys Rev B* 2001;**64**:014104–10.
8. Desgreniers S, Lagarec K. High-density ZrO_2 and HfO_2: crystalline structures and equations of state. *Phys Rev B* 1999;**59**:8467–72.
9. Haines J, Leger JM, Hull S, Petitet JP, Pereira JP, Perottoni CA, et al. Characterization of the cotunnite-type phases of zirconia and hafnia by neutron diffraction and Raman spectroscopy. *J Am Ceram Soc* 1997;**80**: 1910–4.
10. Kim BN, Hiraga K, Morita K, Sakka Y. A high-strain-rate superplastic ceramic. *Nature* 2001;**413**:288–91.
11. Claussen N, Ruhle M. Science and technology of zirconia I. In: Heuer AH, Hobbs LW, editors. *Advances in Ceramics*, vol. 3. Columbus, OH: The American Ceramic Society; 1981. p. 137–63.
12. Mojaki EA. Study of the zirconia–hafnia system and particularly its behaviour at high temperatures and pressures. PhD Thesis. Johannesburg-SA: School of Process and Materials Engineering, University of the Witwatersrand; 2004.
13. Brandau T, Brandau E. Hafnia and hafnia-zirconia mixed oxides ultra spherical microspheres made by a sol–gel-vibrational dropping process. *Key Eng Mater* 1997;**132–136**:38–40.
14. Yoldas BE. Zirconium oxide formed by hydrolytic condensation of alkoxides and parameters that affect their morphology. *J Mater Sci* 1986;**21**:1080–6.
15. Ruh R, Garrett HJ, Domagala RF, Tallen NM. The system zirconia–hafnia. *J Am Ceram Soc* 1968;**51**:23–7.
16. Carlone C. Raman spectrum of zirconia–hafnia mixed crystals. *Phys Rev B* 1992;**45**:2079–84.
17. Krebs MA, Robert A, Condrate SR. Vibrational spectra of HfO_2–ZrO_2 solid solutions. *J Am Ceram Soc* 1982;**65**:C144–5.
18. Witlinger J, Fischer R, Werner S, Schneider J, Schultz H. High-pressure study of h.c.p argon. *Acta Cryst B* 1997;**53**:745–9.
19. Chijioke AD, Nellis WJ, Soldatov A, Silvera IF. The ruby pressure scale to 150 GPa. *J Appl Phys* 2005;**98**:114905–13.
20. Hearne G, Bibik A, Zhao J. CO_2 laser-heated diamond-anvil cell methodology revisited. *J Phys: Condens Matter* 2002;**14**:11531–5.
21. Cornaby S, Szebenyi T, Huang R, Bilderback DH. Design of single-bounce monocapillary X-ray optics. *JCPDS-Int Centre Diffraction Data* 2007:194–200.
22. Bruker. *SMART-NT*. Madison, WI, USA: Bruker AXS Inc.; 1998.
23. Hammersly A. *Computer program FIT2D*. Grenoble: ESRF; 1998.
24. Roisnel T, Rodriguez-Carvajal J. WinPLOTR: a Windows tool for powder diffraction analysis. *Mater Sci Forum* 2001;**378–381**:118–23. See http://www.cdifx.univ-rennes111.fr/winplotr/winplotr.htm.
25. Block S, Piermarini GJ, Hockey BJ, Lawn BR, Munro RG. High-pressure transformation toughening: a case study on zirconia. *J Am Ceram Soc* 1986;**69**:125–6.